



OPEN

## The comprehensive detection of miRNA and circRNA in the regulation of intramuscular and subcutaneous adipose tissue of Laiwu pig

Hui Feng, Salsabeel Yousuf, Tianyi Liu, Xiuxiu Zhang, Wanlong Huang, Ai Li, Lingli Xie & Xiangyang Miao

circRNAs, as miRNA sponges, participate in many important biological processes. However, it remains unclear whether circRNAs can regulate lipid metabolism. This study aimed to explore the competing endogenous RNA (ceRNA) regulatory network that affects the difference between intramuscular fat (IMF) and subcutaneous fat (SCF) deposition, and to screen key circRNAs and their regulatory genes. In this experiment, we identified 265 differentially expressed circRNAs, of which 187 up-regulated circRNA and 78 down-regulated circRNA in IMF. Subsequently, we annotated the function of DEcircRNA's host genes, and found that DEcircRNA's host genes were mainly involved in GO terms (including cellular response to fatty acids, lysophosphatidic acid acyltransferase activity, R-SMAD binding, etc.) and signaling pathways (fatty acid biosynthesis, Citrate cycle, TGF- $\beta$  Signal pathway) related to adipogenesis, differentiation and lipid metabolism. By constructing a circRNA-miRNA network, we screened out DEcircRNA that can competitively bind to more miRNAs as key circRNAs (circRNA\_06424 and circRNA\_08840). Through the functional annotation of indirect target genes and protein network analysis, we found that circRNA\_06424 affects the expression of *PPARD*, *MMP9*, *UBA7* and other indirect target genes by competitively binding to miRNAs such as ssc-miR-339-5p, ssc-miR-744 and ssc-miR-328, and participates in PPAR signaling pathway, Wnt signaling pathway, unsaturated fatty acid and other signaling pathways, resulting in the difference of fat deposition between IMF and SCF. This study provide a theoretical basis for further research investigating the differences of lipid metabolism in different adipose tissues, providing potential therapeutic targets for ectopic fat deposition and lipid metabolism diseases.

### Abbreviations

RNA-seq	RNA sequencing technology
GO	Gene ontology
KEGG	The Kyoto Encyclopedia of Genes and Genomes
IMF	Intramuscular fat
SCF	Subcutaneous fat
DEcircRNAs	Differentially expressed circRNAs
DEmiRNAs	Differentially expressed miRNAs
DEgenes	Differentially expressed target genes of miRNA
PCR	Polymerase chain reaction
PPI	Protein-protein interaction

The amount and distribution of fat deposition in pigs are important factors affecting meat quality<sup>1</sup>. Intramuscular fat (IMF) refers to adipocytes embedded in porcine skeletal muscle tissue. IMF determines the flavor, tenderness and juiciness of the meat, and is an important indicator for the quality of meat<sup>2</sup>. Subcutaneous fat (SCF) mainly

State Key Laboratory of Animal Nutrition, Institute of Animal Sciences, Chinese Academy of Agricultural Sciences, Beijing 100193, China. email: miaoxy32@163.com; mxy32@sohu.com

accumulates in the back and abdomen of pigs. SCF can affect the carcass traits of pigs and is negatively correlated with lean meat percentage<sup>3</sup>. In the breeding process, we expect to breed pigs with high lean meat percentage and high intramuscular fat percentage. It is necessary to reduce subcutaneous fat deposition and increase intramuscular fat deposition. However, there is a high degree of synergy between IM and SC fat deposition in pigs<sup>4</sup>. Therefore, identifying differences in metabolic regulation between adipocytes of the two origins can be helpful for the development of pig breeding that can independently manipulate IM and SC fat deposition.

Adipocyte metabolism is a complex process that is finely regulated by many factors, such as hormones, transcription factors signaling pathways, etc.<sup>5</sup>. Among them, both intramuscular and subcutaneous adipocytes belong to white adipocytes. They are highly similar in the process of differentiation and metabolism, but there are also many differences. Intramuscular adipocytes are mainly derived from bone marrow mesenchymal stem cells (MSCs)<sup>6</sup> and mesenchymal progenitor cells with positive platelet-derived growth factor receptor  $\alpha$  (*PDGFR  $\alpha$* )<sup>7</sup>. Stem cells (SCs), fibroadipocyte precursors (fAPs), fibroblasts, myoendothelial cells, pericytes, hemangioblasts and *PW1* overexpressing cells have been found to serve as sources of intramuscular adipocytes<sup>8,9</sup>. 10–25% of adipocytes in human subcutaneous fat are derived from bone marrow progenitor cells<sup>10</sup>. During adipogenic differentiation, early recruitment of adipocytes is dependent on the regulation of typical Wnt and BMP4 signaling pathways. Wnt signaling pathway enhances the proliferation and differentiation of preadipocytes<sup>11</sup>, while *BMP4* induces the differentiation of preadipocytes into adipocytes<sup>12</sup>. Scholars found that the expression levels of key adipogenic genes, such as peroxisome proliferator-activated receptor gamma (*PPAR  $\gamma$* ) and fatty acid synthase (*FAS*) in intramuscular adipocytes were lower than that in subcutaneous adipocytes. This results in a weaker lipogenic capacity of intramuscular adipocytes than subcutaneous adipocytes<sup>4,13,14</sup>. Some studies have shown that some bioactive substances, such as conjugated linoleic acid, can reduce or maintain the deposition of subcutaneous fat, and increase the content of intramuscular fat<sup>15</sup>. Therefore, the biological function and molecular regulation mechanism of intramuscular fat deposition are different from that of subcutaneous fat. Some studies have shown that circRNA plays a potential regulatory role in the process of adipose metabolism<sup>16</sup>.

Circular RNA (circRNA), an RNA without 5' and 3' polarity<sup>17</sup>, discovered as a class of molecules with functional relevance for the regulation of gene expression<sup>18</sup>. With the continuous development of high-throughput sequencing technology and bioinformatics, researchers have found that circRNAs are widely present in multicellular eukaryotes<sup>19</sup>, such as human (*Homo sapiens*)<sup>20</sup>, mouse (*Mus musculus*)<sup>21</sup>, drosophila (*Drosophila melanogaster*)<sup>22</sup>, *Caenorhabditis elegans* (*Caenorhabditis elegans*)<sup>23</sup>, zebrafish (*Danio rerio*)<sup>24</sup>, rice (*Oryza sativa*)<sup>25</sup>, etc. The circRNA sequences of human, mouse, nematode, speartail and coelacanth were included in the circBase database<sup>26</sup>. circRNA is widely present in mammals with the characteristics of long half-life, conserved sequence structure and tissue-specific expression. At present, the research on the biological function of circRNA have shown that circRNA can regulate the expression of miRNA and reduce the inhibitory effect of miRNA on target mRNA, mainly by acting as the molecular sponge of miRNA<sup>27</sup>. In addition, studies have shown that some circRNA can regulate gene expression by interacting with RNA binding proteins (RBPs)<sup>28</sup>. A large number of studies have shown that circRNAs are related to many diseases, such as Alzheimer's disease<sup>29</sup>, cancer<sup>30</sup>, Cardiovascular and cerebrovascular<sup>31</sup> and neurological disorders<sup>32</sup>; and the process of cell growth and development, for example, cell proliferation<sup>33</sup>, oogenesis<sup>34</sup> and embryonic development<sup>35</sup>.

In this study, we selected Laiwu pigs with high-fat deposition capacity, and obtained their intramuscular fat and subcutaneous adipose tissue. By next-generation sequencing technology, circRNAs and miRNAs were identified in intramuscular and subcutaneous adipose tissue. Gene ontology (GO) and Kyoto Encyclopedia of Genes and Genomes (KEGG) were also used for functional enrichment analyses, circRNAs and miRNAs involved in the regulation of genes related to fat development in Laiwu pigs were identified. We further studied adipogenic gene expression patterns and their enriched pathways in Laiwu Pig to better understand their regulatory roles in adipogenic differentiation and fat metabolism.

## Materials and methods

**Ethics statement.** All procedures involving animals were approved by the Animal Care and Use Committee at Institute of Animal Sciences (Chinese Academy of Agricultural Sciences), where the experiments were performed. All experiments were performed in accordance with guidelines and regulations formulated by the Ministry of Agriculture of the People's Republic of China.

**Experimental animals and sample preparation.** Three 180-day-old Laiwu sows of similar body weight were killed by exsanguination. The subcutaneous fat and intramuscular adipose tissue at the longissimus dorsi muscle were quickly stripped and put into the pre-labeled cryopreservation tubes (L\_PX\_1, L\_PX\_2, L\_PX\_3 and L\_JN\_1, L\_JN\_2, L\_JN\_3. L\_PX represents the subcutaneous adipose tissue of Laiwu pigs, and L\_JN represents the intramuscular adipose tissue of Laiwu pigs). Then, the cryopreservation tubes were placed in liquid nitrogen. Then, they were transported back to the laboratory with dry ice.

**RNA isolation and circRNA sequencing.** We placed the adipose tissues in a mortar pre-cooled with liquid nitrogen and quickly ground it to powder. In order to obtain total RNA, we sequentially added 1 ml TRIzol (Invitrogen Life Technologies, Carlsbad, USA), 0.2 ml chloroform, 0.2 ml isopropanol, 75% ethanol and RNase-free water. The integrity of sample RNA was preliminarily determined by 1% agarose gel electrophoresis. To ensure RNA concentration, we used Nanodrop to detect od260 / 280 and od260 / 230 values. We accurately evaluated the integrity, purity and degradation degree of RNA through Agilent 2100 Bioanalyzer. Six cDNA libraries (L\_PX\_1, L\_PX\_2, L\_PX\_3 and L\_JN\_1, L\_JN\_2, L\_JN\_3) were constructed through TruSeq Stranded Total RNA LT Kit with Ribo-Zero TM Gold (RS-122-2301). The libraries building process includes mRNA enrichment, fragmentation, reverse transcription, double-stranded cDNA synthesis, linker, DNA purifi-

Gene	Forward primer	Reverse primer
circRNA_00907 1:93126380_93142829_+	AGAGTGAGAGGTCTGAATATGATG	CACCACGACAGCCTTGATGA
circRNA_01106 1:110525008_110548336_+	ACCTGGAGATGCTGTTTCATAAGAT	CGGCTAATGTTGCAAGGAAAT
circRNA_06424 12:62458832_62523689_-	GAGCAGAAGCACCGAAGTATTG	TGAACTTGACATTCTCAGGACAGA
circRNA_08840 13:217685619_217779051_-	TGTGTTCTAGATGGAGCCTCT	CGTGGTTAGTTTCTGCGTTGG
circRNA_15332 2:59187624_59255661_+	GATGAGACCAACGACGAGGAG	TCAGAGCTGCTGTAGACCTTG
circRNA_22410 6:92745097_92803482_+	GGCATCTTGCTGTTTCGTGATTA	ATGGTCTCCTCCGCTTCTTG
miR-328	CCCTCTCTGCCCTTCCGT	
miR-361-3p	CCAGGTGTGATTCTGATTTCG	
miR-331-3p	CCCCTGGGCCTATCCTAGAA	
PPARD	CGAGTTCGCCAAGAGCATCC	GCACGCCGTACTTGAGAAGG
MMP9	TGTTAAGGAGCACGGAGATGG	TGGCGGTCGGTGCATAGT

**Table 1.** Gene and the corresponding primer sequences.

cation and PCR amplification. To test the length and quality of the library, we added samples to the Agilent 2100 biological analyzer. After the quality inspection is qualified, samples were sequenced by Illumina HiSeqTM2500 platform.

**circRNA identification and differential analysis.** We first adopted paired-end sequencing. After obtaining sequencing data, we used NGSQC Toolkit (v2.3.3) for quality control and adapter trimming (Keep default parameters). Then, low-quality bases and N-bases were trimmed from the reads. Finally, high-quality clean reads were obtained for subsequent analysis. CIRI<sup>36</sup> was used to identify circRNAs. DEseq2<sup>37</sup> was used for differential expression analysis of circRNAs.  $|\log_2\text{FoldChange}| \geq 1$  and  $P\text{-value} \leq 0.05$  were used to indicate significant difference in circRNA expression between treatment groups and the control group. Using the intersectbed software<sup>38</sup>, we obtain the protein-coding transcript with the largest overlapping region of circRNA in the genome, that is, the host gene of circRNA, based on the number of cyclization sites in the transcript region and the number of exons between the shear sites.

**Bioinformatics analysis and target gene prediction.** We performed miRNA target prediction for circRNAs using MiRanda software<sup>40</sup>. To explore the potential functions of circRNAs in adipose tissue, we selected circRNAs that can competitively bind more miRNAs as key circRNAs, and analyzed the sequence of key circRNAs. The open reading frames (ORFs) of circRNA were predicted by ORFinder ([http://www.bioinformatics.org/sms2/orf\\_find.html](http://www.bioinformatics.org/sms2/orf_find.html)). The prediction results were input into the Conserved Domains database (<https://www.ncbi.nlm.nih.gov/Structure/cdd/wrpsb.cgi>) to predict the protein-coding ability of ORFs of circRNA.

**GO and KEGG enrichment and protein–protein interaction network analysis.** We performed GO (gene ontology, <http://www.geneontology.org>) and KEGG (Kyoto encyclopedia of genes and genomes, <http://www.genome.jp/kegg>) enrichment analysis on the host and indirect target genes of circRNA using clusterProfiler package<sup>41</sup> in R software, and  $P\text{-value} \leq 0.05$  was significant enrichment. The enrichment results were shown in bar graphs and bubble graphs.

We selected circRNAs that can bind to more miRNAs as key circRNAs. Taking the differentially expressed genes targeted and regulated by the key circRNA, we applied the STRING database to analyze the protein interaction network. Then, we input the prediction results with a comprehensive score greater than 0.4 (medium) into the cytoscape software for visual display.

**Validation of real-time fluorescence quantitative PCR.** 6 circRNAs (circRNA\_00907, circRNA\_01106, circRNA\_06424, circRNA\_08840, circRNA\_15332 and circRNA\_22410), 3 miRNAs (miR-328, miR-361-3p and miR-331-3p) and 2 genes (PPARD and MMP9) were randomly selected for qRT-PCR validation experiment to ensure the accuracy of sequencing data. qRT-PCR was performed in triplicate, and total RNA was extracted from tissue samples using the Total RNA Extraction Kit (DNase I) kit (GenePool, Cat# GPQ1801). Then, reverse transcription was performed with circRNA cDNA Synthesis Kit (GenePool, Cat# GPQ1805), miRNA cDNA Synthesis Kit (GenePool, Cat# GPQ1804) and mRNA cDNA Synthesis Kit (GenePool, Cat# GPQ1803). We performed quantitative analysis of data through Bioer linegene 9600plus fluorescence quantitative PCR instrument and  $2^{-\Delta\Delta C_t}$  method<sup>42</sup>, detailed in Table 1. At the same time, the melting curve analysis was performed at 60–95 °C, and the standard curve of the target gene was drawn.

**miRNA and mRNA sequencing.** We obtained the sequencing results of circRNA, miRNA and mRNA in the same experiment. The results of miRNAs and mRNAs have been published in "Frontiers in Veterinary Science" (<https://www.frontiersin.org/articles/10.3389/fvets.2022.976603/full>).

Sample	Raw reads	Clean reads	Valid bases (%)	Q30 (%)	GC (%)
Sample_L_JN_1	80013516	77555412	96.76	92.25	63
Sample_L_JN_2	79818561	77374868	96.78	92.37	61
Sample_L_JN_3	79623606	77194324	96.80	92.49	59
Sample_L_PX_1	79432576	75995332	95.46	90.38	66.50
Sample_L_PX_2	79473958	75914582	95.28	90.44	66.50
Sample_L_PX_3	79526364	76470692	95.98	91.52	61.50

**Table 2.** Summary of reads of Laiwu Pig transcriptome. L\_JN\_1-3 refers to intramuscular adipose tissues; L\_PX\_1-3 refers to subcutaneous adipose tissues.

**Statistical analysis.** All data are presented as mean  $\pm$  standard. A student's t-test was performed for comparisons by excel,  $p < 0.05$  was statistically significant.

**Ethics approval.** The experimental procedure was approved and supervised by the Animal Care Commission of the Institute of Animal Sciences, Chinese Academy of Agricultural Sciences. All experiments were performed in accordance with guidelines and regulations formulated by the Ministry of Agriculture of the People's Republic of China.

## Results

**Reads mapping transcriptome and quality control.** The original data in L\_PX and L\_JN were subjected to quality control, and the clean reads results were shown in Table 2.  $Q30 \geq 90\%$  and  $GC \geq 61\%$  in 6 samples indicated reliable sequencing results. We compared clean reads with reference genes, and identified 29,763 circRNAs. The length distribution of circRNAs sequences and the number of exons were shown in Fig. 1A,B, respectively. The length of these circRNAs sequences was mainly between 201 and 600 bp, and the content of exons was mainly from 1 to 5. Based on rpm values of circRNAs expression, we constructed an RPM box Whistler plot, as shown in Fig. 1C. The expression of circRNAs in intramuscular adipose tissue was higher than that in subcutaneous tissue.

**Identification of differentially expressed circRNA.** There are significant differences between subcutaneous fat and intramuscular fat deposition of pigs, and the expression of circRNAs is tissue-specific. Through the differential expression analysis of circRNA, we screened 265 differentially expressed circRNAs, including 187 up-regulated and 78 down regulated in IMF. The differential expressions of 104 DEcircRNAs were more than 4 times, as shown in Fig. 2A. The specific expression of DEcircRNA was analyzed. 44 DEcircRNAs were specifically expressed in L\_PX, 109 DEcircRNAs were specifically expressed in L\_JN, and 112 DEcircRNAs were expressed in both tissues, as shown in the Venn diagram of Fig. 2B. 4 antisense, 7 exonic, 66 intergenic and 188 sense-overlapping circRNAs identified among 265 DEcircRNAs, as shown in Fig. 2C.

**Functional annotation of circRNA host genes.** A large number of studies have shown that circRNA can affect the transcription of host genes. Therefore, we performed GO and KEGG (Fig. 3) enrichment annotations of the host genes of DEcircRNAs. The host genes of DEcircRNAs were significantly involved in 638 GO terms, of which a large number of GO terms were related to fat deposition and metabolism (Fig. 3A). In biological process, host genes were mainly involved in cellular response to fatty acid, glycogen catabolic process, nucleotide phosphorylation, phospholipase C-activating angiotensin-activated signaling pathway, positive regulation of lipid catabolic process. From the perspective of cell composition, host genes are mainly involved in mitochondrial pyruvate dehydrogenase complex, phosphatidylinositol 3-kinase complex, class III, phosphatidylinositol 3-kinase complex, class III, type I, phosphatidylinositol 3-kinase complex, class III, type II, SMAD protein complex. From the perspective of molecular functions, host genes are mainly involved in 4-alpha-glucanotransferase activity, amylo-alpha -1,6-glucosidase activity, galactokinase activity, glycogen debranching enzyme activity, etc. The differentially expressed circRNA was significantly involved in 28 signal pathways with  $P\text{-value} \leq 0.05$  (Fig. 3B). Among them, the Citrate cycle (TCA cycle), Propanoate metabolism, Phenylalanine metabolism, Pyruvate metabolism, Fatty acid biosynthesis, TGF- $\beta$  signaling pathways and other signaling pathways are already proven as signaling pathways related to fat deposition and metabolism.

**Bioinformatics analysis and target gene prediction.** As a non-coding RNA, current research shows that circRNA plays a regulatory role mainly through competitive binding of miRNAs, thereby affecting the biological functions of miRNAs. Therefore, the miRNA regulated by DEcircRNA is important in this experiment. The target miRNAs of DEcircRNAs were predicted using miRanda software. Taking the circRNA-miRNA relationship pair of top300, we used the cytoscape software to draw the circRNA-miRNA regulatory network diagram. In Fig. 4, circRNA\_08840 can bind 43 miRNAs, and circRNA\_06424 can bind 25 miRNAs, which are the two circRNAs that can bind the most miRNAs. So the down-regulated circRNA\_06424 and the up-regulated circRNA\_08840 in the regulatory network can serve as molecular sponges for more miRNAs with a

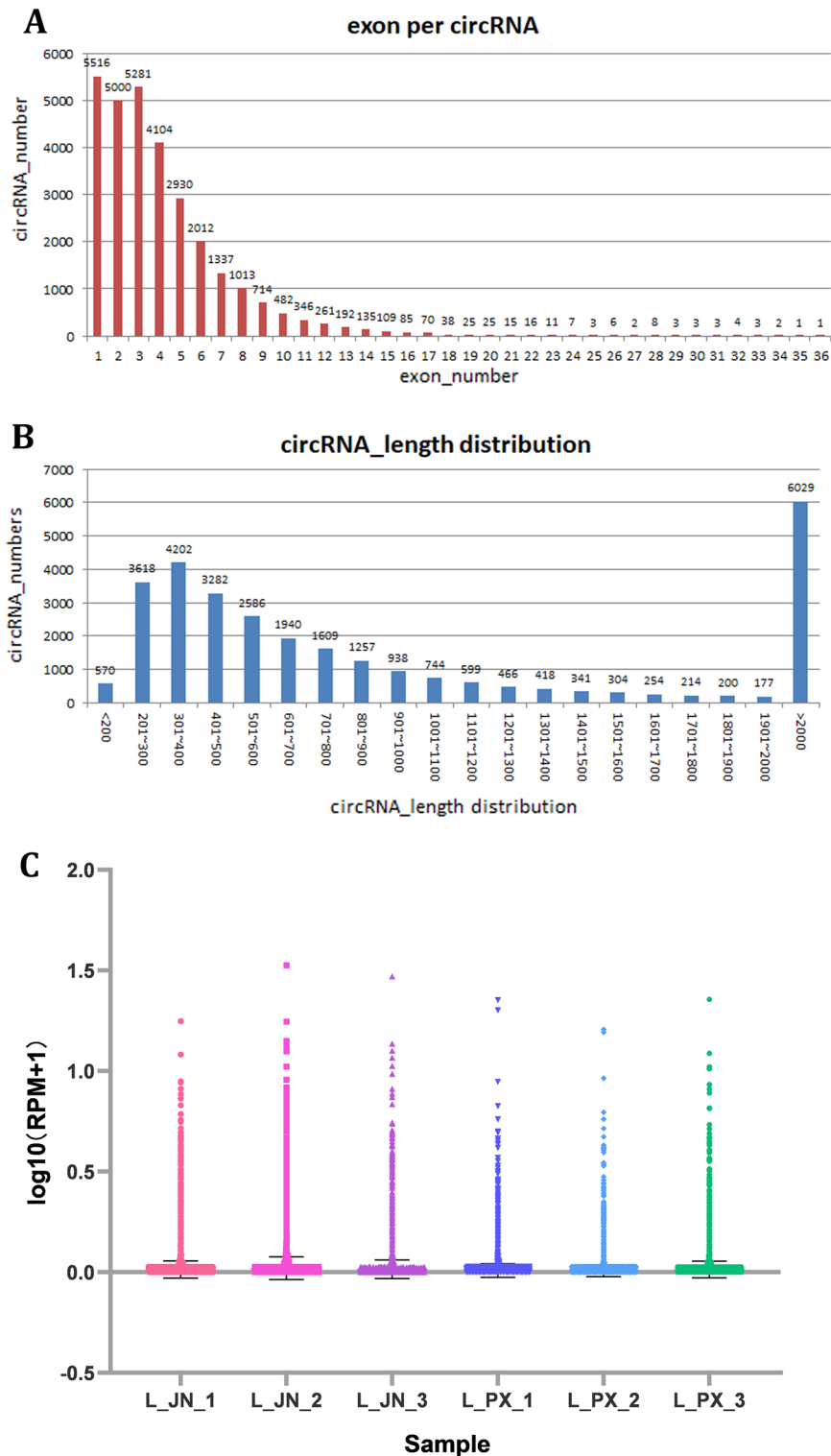


**Figure 1.** Overview of circRNAs in the L\_JN and L\_PX. (A) circRNA length distribution. (B) Exon content. (C) Expression level.

key role in adipogenic differentiation and lipid metabolism. In addition, DEcircRNAs, such as circRNA\_19382, circRNA\_15332, circRNA\_15525, circRNA\_21469 can also regulate many miRNAs.

**Key circRNAs sequence analysis.** Several human circRNAs had translation capabilities and played a key role in tumors and cancers<sup>43</sup>. By constructing the circRNA-miRNA regulatory network, we screened the key circRNA\_06424 and circRNA\_08840. We found that circRNA\_06424 and circRNA\_08840 are both sense-over-

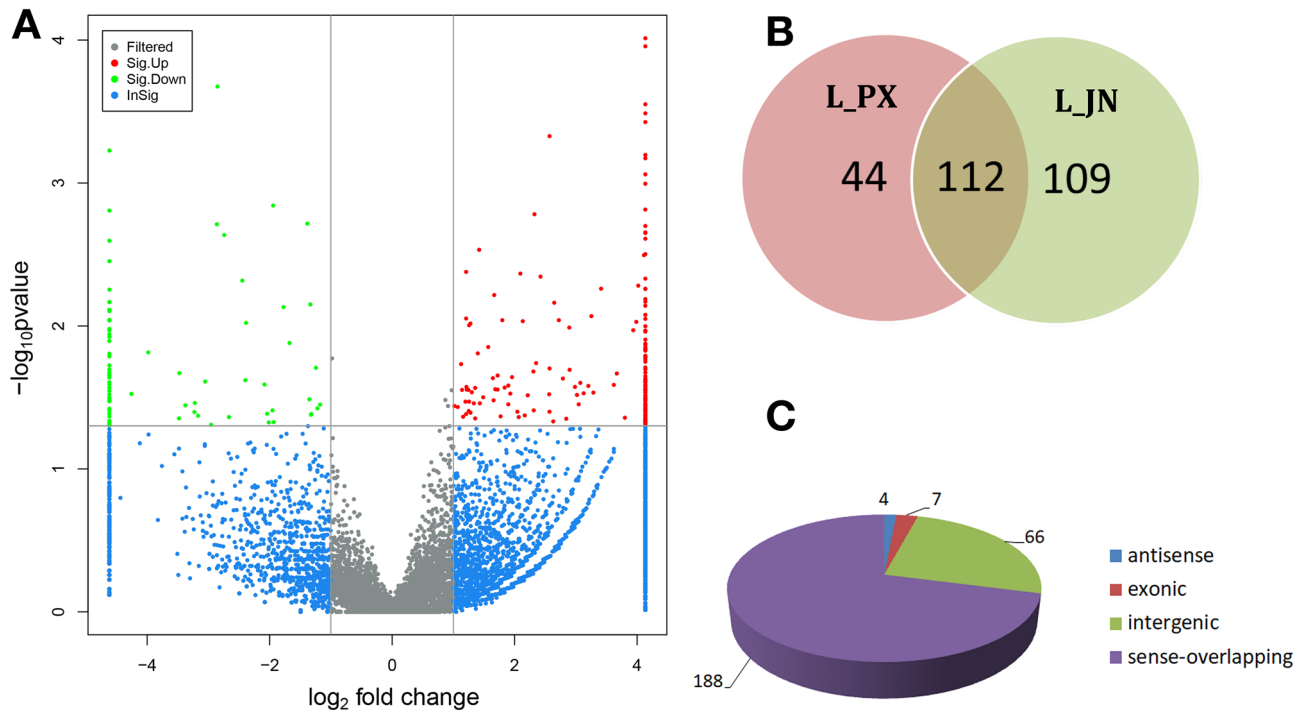


**Figure 2.** Overview of DEcircRNAs in the L\_JN and L\_PX. **(A)** Volcano plots showing the distribution of differentially expressed circRNAs between two adipose tissues. **(B)** Specific expression circRNA. **(C)** The proportion of various circRNAs in total DEcircRNAs.

lapping circRNAs, which are transcribed from gene regions with potential coding capabilities. circRNA\_06424 has a sequence length of 64858 bp and is located on pig chromosome 12, derived from *ENSSSCG000000180391*. circRNA\_08840 has a sequence length of 93433 bp, is located on chromosome 13 of pigs, and derived from *ADARB*. The results of ORFinder Prediction shows that there are 254 and 342 open reading frames (ORFs) in circRNA\_06424 and circRNA\_08840, respectively. We predicted the potential coding ability of Conserved Domains for these ORFs. The results are shown in Tables 3 and 4.

**Competing endogenous RNA (ceRNA) network.** circRNA binds miRNA competitively with mRNA, thereby reducing the inhibitory effect of miRNA on mRNA, and increasing the expression of indirect target genes. The ceRNA regulatory network is usually constructed by DEcircRNA-DEmiRNA-DEgene to explore the function of circRNA. In this study, we selected circRNA\_06424 and circRNA\_08840 target miRNAs with higher expression and its target DEgenes, to construct a ceRNA network (Fig. 5). In the ceRNA network centered on circRNA\_06424, there are 7 down-regulated DEmiRNAs and 52 DEgenes with higher expression levels. In the ceRNA network centered on circRNA\_08840, there are 8 DEmiRNA and 44 DEgene. circRNA\_06424 and circRNA\_08840 have three common target miRNAs (*ssc-miR-339-5p*, *ssc-miR-744*, *ssc-miR-328*).

**Function annotation of intircet target genes.** We found the genes targeted and regulated by the key circRNA through the construction of the ceRNA network. To further explore the function of circRNA, we performed GO and KEGG enrichment analysis on the indirect target genes of the key circRNAs. The indirect target genes of CircRNA\_06424 were significantly involved in 160 GO terms, and the top30 GO terms were selected, as shown in Fig. 6A. Among them, GO terms related to fat deposition and metabolism are fatty acid binding, phosphatase inhibitor activity, positive regulation of phosphatidylinositol 3-kinase signaling. There are GO terms related to cell differentiation, such as negative regulation of myoblast differentiation. In Fig. 6C, KEGG enrichment analysis revealed that the indirect target genes of circRNA\_06424 are involved in the signaling pathways related to lipogenesis and metabolism in Biosynthesis of unsaturated fatty acids, PPAR signaling pathway, and Wnt signaling pathway. In addition, a large number of studies have shown that lipid production and metabolism will also change in patients with immune reactions. Therefore, signal pathways such as Chagas disease, Human immunodeficiency virus 1 infection, and Hepatitis B also need attention in the difference between subcutaneous and intramuscular fat deposition. The indirect target genes of circRNA\_08840 were significantly involved in 134 GO entries. The top 30 GO terms were selected, as shown in Fig. 6B. Many of these GO terms were related to fat deposition and metabolism, such as positive regulation of phosphatidylinositol 3-kinase signaling, inositol lipid-mediated signaling, negative regulation of myoblast differentiation. The KEGG results (Fig. 6D) showed that these indirect target genes are involved in Wnt signaling pathway, Insulin signaling pathway, PPAR signaling pathway, and some disease-related signaling pathways, such as Hepatitis B, TNF signaling pathway, mTOR signaling pathway.

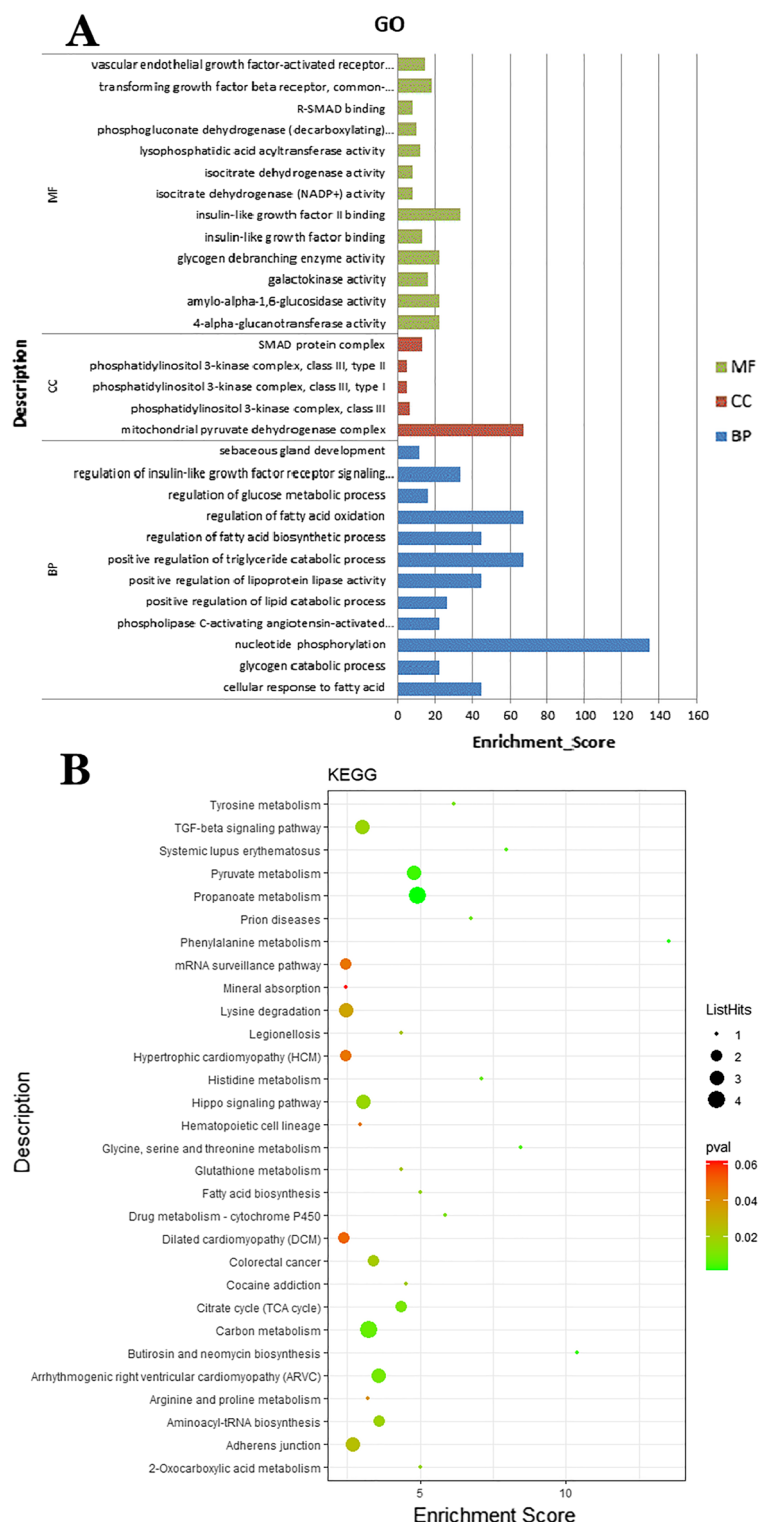


**Figure 3.** Function annotation of host genes. **(A)** GO enrichment analysis. **(B)** KEGG pathway analysis. The x-axis represents the enrichment\_score, the y-axis represents the name of the GO terms or pathways.

**Protein–protein interaction (PPI) network.** Studying the interaction network between proteins can find out the core regulatory genes. In this experiment, we studied the protein interaction relationship between the key circRNA indirect target genes identified in L\_JN and L\_PX, and used the degree value of each protein as a screening index to draw a PPI network diagram, as shown in Fig. 7. *PPARD*, *CHD5*, *CDK16*, *UBA7*, *EHMT2*, *ARLAD*, *SUPT5H* and *HUWE1* are at key nodes of the PPI network, and can interact strongly with more pro-

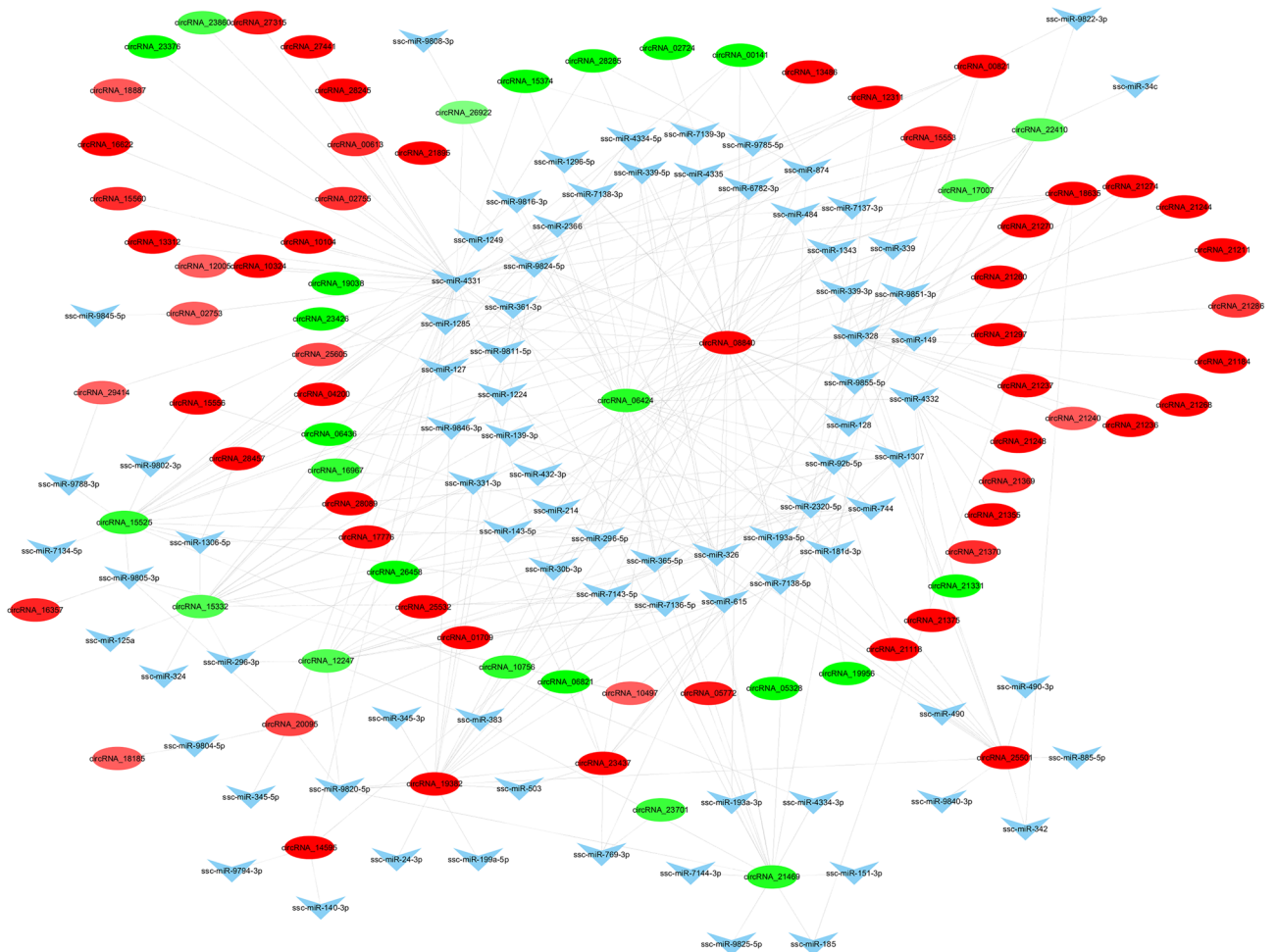


**Figure 4.** circRNA-miRNA interaction network. The circle represents the circRNA; triangle represents the miRNA; red represents upregulation; green represents downregulation; blue represents no difference.

Query	PSSM-ID	From	To	E-Value	Bitscore	Accession	Short name
ORF 198	240654	3	36	0.005757	31.5226	cd12177	2-Hacid_dh_12
ORF 198	419666	3	36	0.005757	31.5226	cl21454	NADB_Rossmann superfamily
ORF 222	223021	21	112	0.008785	36.0697	PHA03247	PHA03247
ORF 222	223021	21	112	0.008785	36.0697	cl33720	PHA03247 superfamily

**Table 3.** circRNA\_06424 sequence ORFs coding ability prediction information.

Query	PSSM-ID	From	To	E-Value	Bitscore	Accession	Short name
ORF 62	237973	2	33	0.002159	32.3316	cl36492	PRK15488 superfamily
ORF 80	223021	3	291	0.009692	37.9957	cl33720	PHA03247 superfamily
ORF 128	237865	97	206	0.001266	40.0828	cl36447	PRK14951 superfamily
ORF 216	411326	41	67	0.00088	38.5856	cl41408	NlpC_p60_RipA superfamily
ORF 232	419665	1	30	0.001868	32.6703	cl21453	PKc_like superfamily
ORF 245	413469	17	58	0.002999	34.0771	cl02775	Oxidoreductase_nitrogenase superfamily

**Table 4.** circRNA\_08840 sequence ORFs coding ability prediction information.

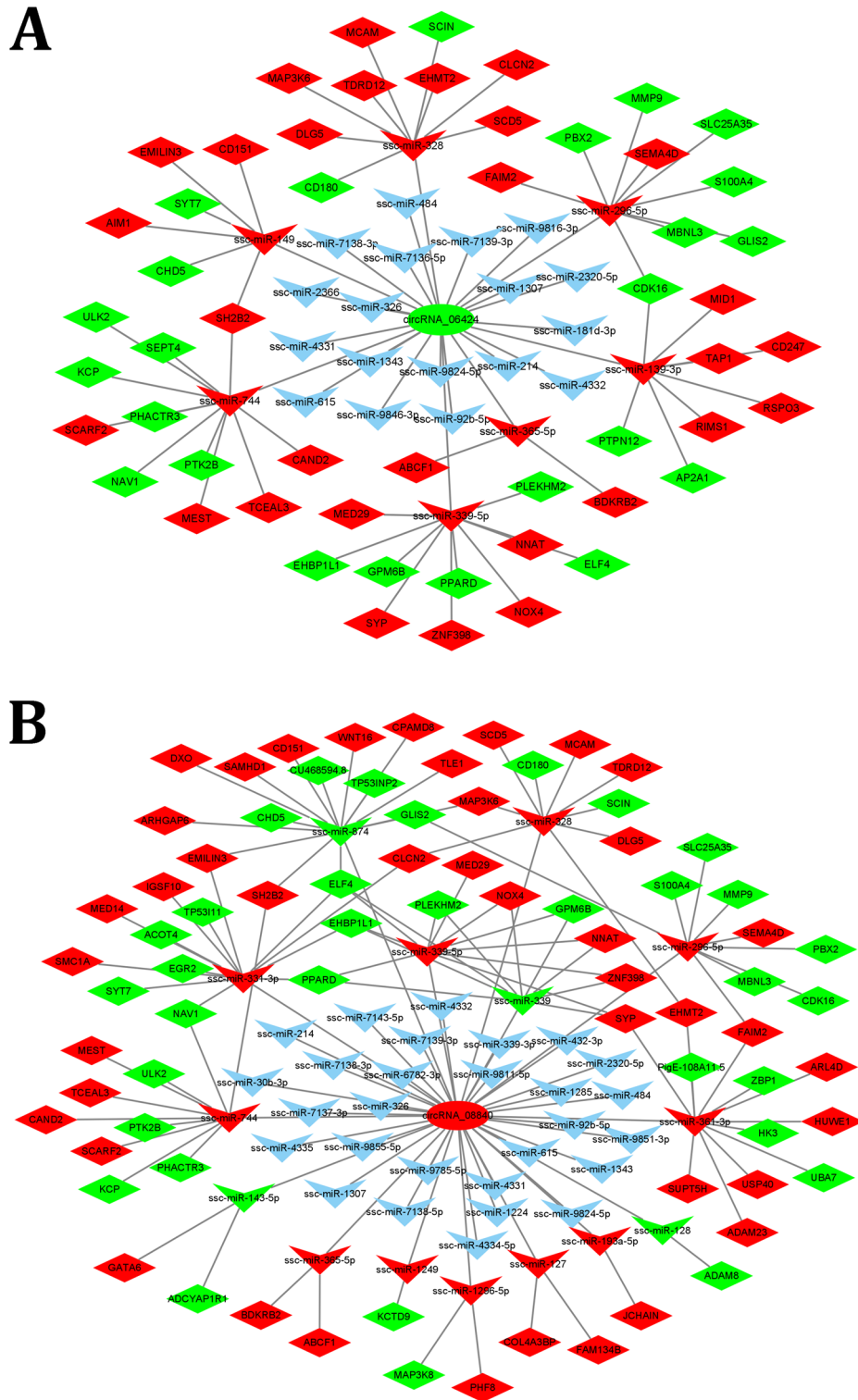


**Figure 5.** ceRNA networks of (A) circRNA\_06424 and (B) circRNA\_08840. Circle represents circRNA; triangle represents the miRNA; diamond represents gene; red represents up-regulation; green represents down-regulation; blue represents no difference.

teins. This indicates that these proteins can play an important role in the significant difference between IMF and SCF deposition levels.

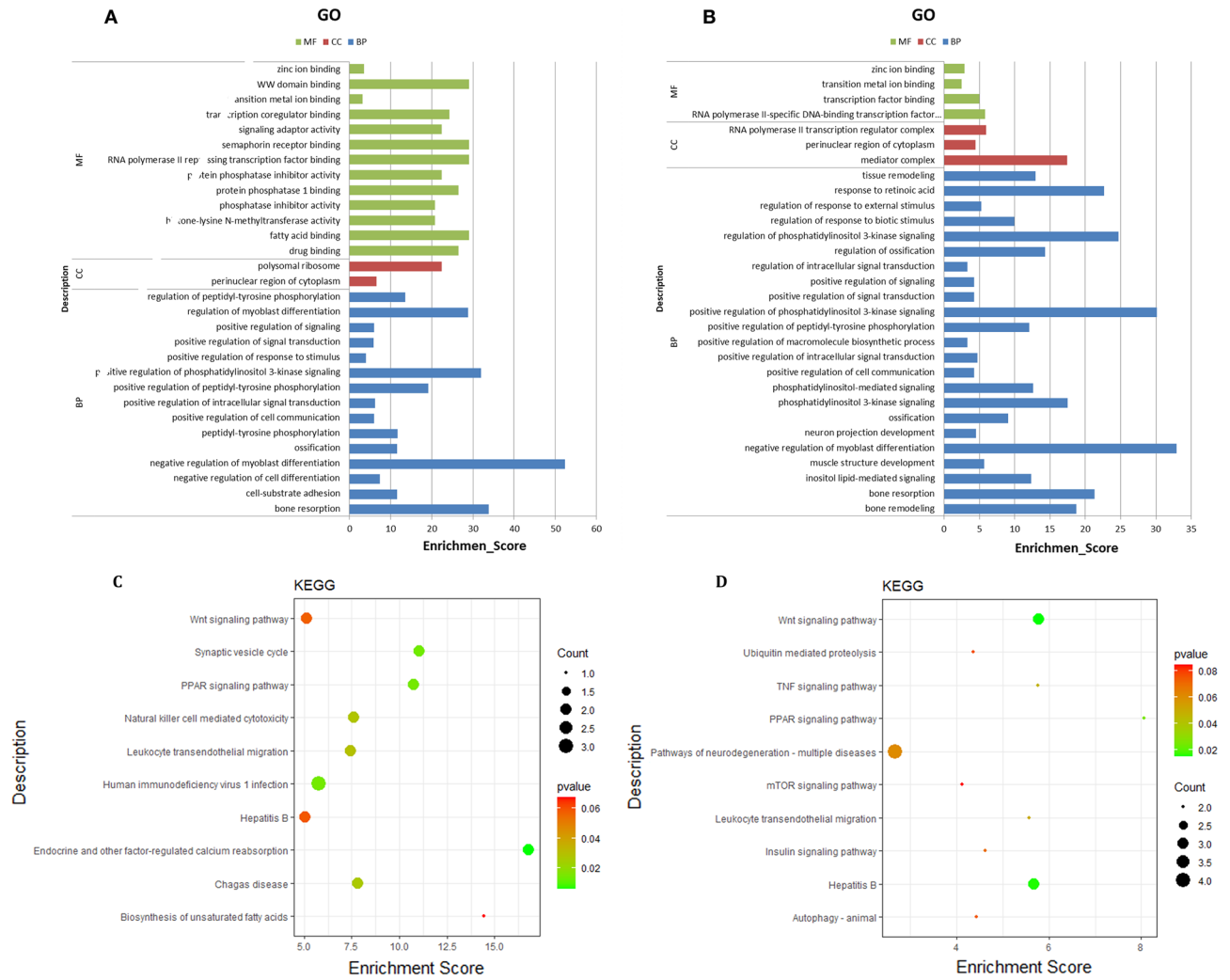


**Figure 6.** GO analysis of target genes of (A) circRNA\_06424 and (B) circRNA\_08840. KEGG pathway analysis of target genes of (C) circRNA\_06424 and (D) circRNA\_08840.

**qRT-PCR verification.** According to the original detection results of Real Time PCR and the relative quantitative calculation formula of  $2^{-\Delta\Delta CT}$ , we calculated the relative quantitative results of the indirect target genes of each sample, as shown in Fig. 8. The gene standard curve and dissolution curve showed that R2 reached 0.99, indicating that the linear correlation was very high, and the amplification efficiency was above 90%, indicating that the experiment was effective (Supplementary material). The q-PCR results are consistent with the sequencing results. This indicates that the sequencing results are true and reliable.

### Discussions

In this experiment, L\_PX was used as the control group, and L\_JN was the experimental group. A total of 265 differentially expressed circRNAs were identified, of which 178 were up-regulated and 87 were down-regulated. Since most circRNAs come from exon regions within protein coding genes, circRNA can inhibit the expression of host genes<sup>39</sup>. Since the circular structures of circRNAs covalently linked are stable, they have a longer half-life. Most circRNAs perform biological functions by acting as molecular sponges for miRNAs<sup>44</sup>. Therefore, we annotated the host gene function of DEcircRNA, the molecular sponge of miRNA, and ceRNA regulation networks, and used the circRNA-miRNA-mRNA axis to analyze the potential regulatory functions of circRNA.

In this study, we annotated the host genes of circRNA, and found that the host genes were mainly involved in SMAD protein complex and other GO terms related to fat deposition and metabolism. The result of KEGG enrichment analysis showed that host genes were mainly involved in TGF-beta signaling pathway.

The phosphorylation of the SMADs family can activate TGF-β Signaling pathway<sup>45</sup>. TGF-β can inhibit the differentiation of 3T3-F442A cells into adipocytes through SMAD3 signal pathway<sup>46</sup>. The transforming growth factor β (TGF β) superfamily consists of more than 33 members, including t TGF βs, BMPs, GDFs, activating, and nodule-associated proteins<sup>47</sup>. BMPs and TGF-β bind to the receptor protein to form complexes that specifically activates and phosphorylates SMADs protein. The phosphorylated SMADs protein binds with SMAD4 to form complexes and transfer to the nucleus, thereby regulating gene transcription<sup>46</sup>. TGF-β-SMAD2/3 signal



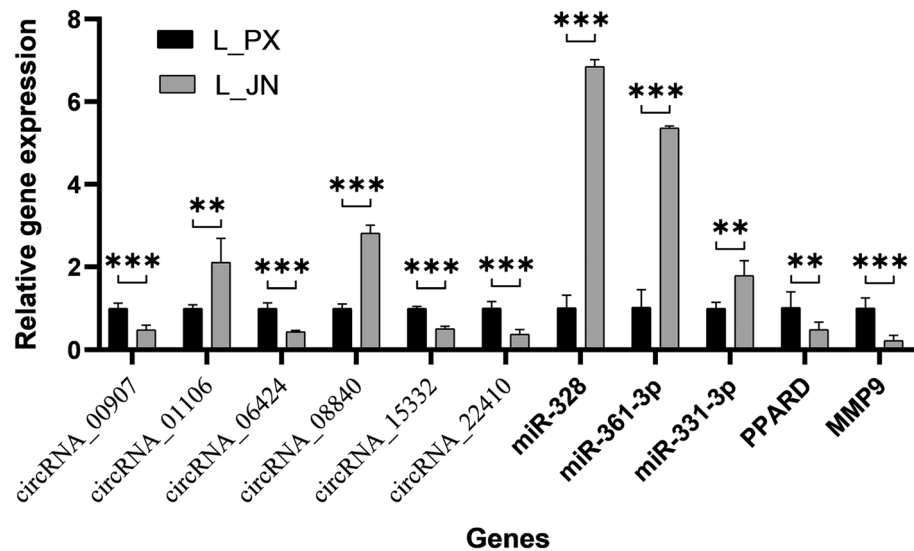


**Figure 8.** qRT-PCR verification results. The differential expression of genes between intramuscular and subcutaneous adipose tissue in Laiwu pig was verified qRT-PCR. \* $p < 0.05$ ; \*\* $p < 0.01$ ; \*\*\* $p < 0.001$ .

preadipocytes with over-expressing miR-128 plasmid under glucocorticoid treatment (with miR-SC and miR-128 inhibitors as the control group). The results showed that the level of triglycerides was significantly increased. The further analysis showed found that miR-128 caused lipid accumulation by inhibiting the expression of *SIRT1*<sup>53</sup>. The expression of miR-128 was down-regulated in L\_JN. This is consistent with the results of existing studies. Wang et al. selected Huainan pig and Duroc as experimental materials and constructed a ceRNA regulatory network. They found that miR-874 is closely related to adipogenesis<sup>54</sup>. circRNA\_08840 can regulate the level of lipid deposition through binding with target miRNAs.

The results showed that some miRNAs, such as miR-328, miR-296-5p, miR-365-5p, miR-339-5p, and miR-774, can simultaneously bind to circRNA\_08840 and circRNA\_06424. It has been found that metabolic disorders can present in cancer patients, especially in lipid metabolism. Therefore, some scholars believe that abnormally metabolized lipids are markers of cancer<sup>55</sup>. Numerous studies have shown that miR-328 exerts the anti-tumor effect by regulating target genes and downstream pathways<sup>56,57</sup>. The overexpression of miR-328-3p can aggravate the oxidative stress injury of endothelial cells in the arterial valve<sup>58</sup>. MiR-328 can reduce inflammation, apoptosis, and oxidative stress of endothelial cells induced by oxidized low-density lipoprotein (Ox-LDL) by specifically binding to *HMGB1*<sup>59</sup>. Overexpression of miR-328 can inhibit the expression of *PTEN* and inhibit the activation of PI3K-Akt signaling pathway<sup>60</sup>. The activity of PI3K-Akt signal pathway was decreased, and glucose absorption was decreased, thereby regulating lipid metabolism. The overexpression of miR-328 can inhibit *BACE1* translation, increase glucose metabolism, promote lipid accumulation in muscle progenitor cells, and promote the differentiation of brown adipocytes and brown adipocytes<sup>61</sup>. In human adipose hepatocytes, miR-296-5p can target the 3'UTR of *PUMA* and reduce the expression of *PUMA*, thereby reducing lipotoxicity and adipocyte apoptosis<sup>62</sup>. Belarbi compared the activity of *EBF1* and differentially expressed miRNA in the white fat (WAT) of obese women and non-obese women. They found that mi-365-5p was expressed at a high level in obese women's WAT and could target and regulate *BEF1* and overexpress miR-365-5p can reduce the activity of *EBF1* and cause white fat hypertrophy<sup>63</sup>.

In this study, we performed functional annotation analysis of the ceRNA network centered on circRNA\_06424 and circRNA\_08840. The results showed that the indirect target genes of circRNA\_06424 were mainly involved in the positive regulation of phosphatidylinositol 3-kinase signaling, phosphatase inhibitor activity, fatty acid binding, and other related GO terms related to lipogenesis and metabolism. The results of KEGG showed that the indirect target genes of circRNA\_06424 were mainly involved in signaling pathways, such as Biosynthesis of unsaturated fatty acids, PPAR signaling pathway, and Wnt signaling pathway. These signaling pathways are classic signaling pathways that regulate fat deposition metabolism. This is similar to the results of the functional annotation analysis of the ceRNA regulatory network with circRNA\_08840. Wnt signal pathway was divided into classical Wnt signal pathway and atypical Wnt signal pathway<sup>64</sup>. Typical Wnt signaling pathway can enhance preadipocyte proliferation<sup>65</sup> and inhibit the differentiation of preadipocytes into adipocytes<sup>66</sup>. The atypical Wnt signaling pathway can inhibit PPAR transcription in bone marrow mesenchymal stem cells, thereby inhibiting the differentiation of mesenchymal stem cells into adipocytes<sup>67</sup>. However, some studies have shown that atypical Wnt signal pathway ligand *WNT5B* can promote adipogenesis by inhibiting the typical Wnt signaling pathway when adipogenic precursors are stimulated by adipogenesis<sup>68</sup>.

We have verified the function of ceRNA network, which can play an important regulatory role in lipogenesis and metabolism. Similarly, we found that the indirect target gene of novel circle RNA is at a key position in the PPI network, especially *PPARD*. Osmotic proliferator-activated receptor family (PPARs) are lipid-activating factors that play multiple roles in fat development and metabolism. The main function of *PPARD* is to directly

or activate related genes to regulate adipogenesis and lipid metabolism. *PPARD* agonists in mice can alleviate obesity caused by high-fat diet. In vitro experiments, activating *PPARD* in adipocytes can promote fatty acid oxidation and utilization<sup>69</sup>. Overexpression of *PPARD* in brown adipose tissue increases lipid droplet consumption<sup>69</sup>. It can also induce the expression of *UCPI* (a marker gene of brown fat). *PPARD* can also participate in fatty acid metabolism in skeletal muscle<sup>70,71</sup>. Mouse myoblasts overexpressing porcine *PPARD* can inhibit the formation of myotubes in vitro. When *PPARD* and *PPARG* are co-expressed, they can promote the expression of fatty acid-binding protein (aP2) and other adipogenic genes in the cell, resulting in a large accumulation of triglycerides<sup>72</sup>. Cytokines secreted by adipocytes can induce *PPARD* expression, thereby inducing alternate activation of macrophages<sup>73</sup>. Adipocytes and macrophages use intercellular mitochondrial transfer to participate in the metabolic homeostasis, including promoting the glucose utilization of by adipocytes, regulating lipid storage, and increasing energy consumption<sup>74</sup>. *PPARD* directly enhances the transcriptional activity of *MMP9* and promotes umbilical vein endothelial cell (EPCS) and C2C12-grade cell differentiation by activating the *PPARD*-*MMP9*-*IGF-1* axis<sup>75</sup>. However, EPCS and C2C12 were cultured in vitro under certain specific conditions with the potential to differentiate into intramuscular fat<sup>76,77</sup>. *MMP9* can degrade the basement membrane<sup>78</sup>, thereby promoting the invasion of macrophages into fat cells. In addition, the expression of *MMP9* was correlated with the level of low-density lipoprotein sterol<sup>79</sup>, lipid metabolism and lipid uptake<sup>80</sup>, visceral obesity<sup>81</sup>, atherosclerotic lesions<sup>82</sup>, diabetes and tumors<sup>83</sup>, and other lipogenesis and metabolism diseases. The research on *PPARD* shows that the single nucleotide polymorphism (SNP) of *PPARD* has a great impact on its function<sup>84,85</sup>. For example, RS6902123 is an SNP significantly associated with type 2 diabetes<sup>86</sup>. In this study, compared with other genes, the expression of *PPARD* was higher. And the expression of *PPARD* in SCF was significantly higher than that in IMF. The amount of IMF and SCF in Laiwu pigs were significantly higher than that of other breeds of pigs. *PPARD* has different mechanisms of action on fat deposition in different parts of Laiwu pigs, which may be related to the interaction of related genes and SNP<sup>87</sup>. Nonetheless, the exact mechanism of action is uncertain. *PPARD* plays an important role in fat deposition<sup>87</sup>. This is consistent with the results of existing studies. CircRNA\_06424 can regulate the expression of *PPARD* through the competitive binding of miRNA with the mRNA. This is the reason for the different regulatory mechanisms of *PPARD* in IMF and SCF.

## Conclusions

In sum, this study used circRNA sequencing and bioinformatics technology to analyze the expression of circRNAs in the subcutaneous and intramuscular adipose tissues of Laiwu pigs for the first time. A total of 265 differentially expressed circRNAs were identified in the subcutaneous adipose tissue. Among them, 178 were up-regulated and 87 were down-regulated in the subcutaneous adipose tissue. CircRNA-miRNA target prediction was performed, and a circRNA-miRNA-mRNA interaction network was constructed. Through GO and KEGG pathway analyses, we found that these indirect target genes and host genes of differentially expressed circRNAs were involved in adipogenic differentiation and lipid metabolism, as well as disease-related pathways. This indicates that circRNAs can regulate adipogenic differentiation and lipid metabolism. This study provides a theoretical basis for further study on the mechanism of fat deposition, providing potential therapeutic targets for metabolism related diseases.

## Data availability

All data were presented in the main manuscript and are available to readers.

Received: 6 May 2022; Accepted: 22 September 2022

Published online: 03 October 2022

## References

- Zhou, G. *et al.* Global comparison of gene expression profiles between intramuscular and subcutaneous adipocytes of neonatal landrace pig using microarray. *Meat. Sci.* **86**(2), 440–450 (2010).
- Alfaia, C. M. *et al.* Current feeding strategies to improve pork intramuscular fat content and its nutritional quality. *Adv. Food Nutr. Res.* **89**, 53–94 (2019).
- Nonneman, D. J. *et al.* Genome-wide association of meat quality traits and tenderness in swine. *J. Anim. Sci.* **91**(9), 4043–4050 (2013).
- Sun, W. X. *et al.* Global comparison of gene expression between subcutaneous and intramuscular adipose tissue of mature Erhualian pig. *Genet. Mol. Res.* **12**(4), 5085–5101 (2013).
- Cristancho, A. G. & Lazar, M. A. Forming functional fat: A growing understanding of adipocyte differentiation. *Nat. Rev. Mol. Cell Biol.* **12**(11), 722–734 (2011).
- Du, M. *et al.* Meat science and muscle biology symposium: Manipulating mesenchymal progenitor cell differentiation to optimize performance and carcass value of beef cattle. *J. Anim. Sci.* **91**(3), 1419–1427 (2013).
- Uezumi, A. *et al.* Identification and characterization of PDGFRalpha+ mesenchymal progenitors in human skeletal muscle. *Cell Death Dis.* **5**, e1186 (2014).
- Geloen, A., Roy, P. E. & Bukowiecki, L. J. Regression of white adipose tissue in diabetic rats. *Am. J. Physiol.* **257**(4 Pt 1), E547–E553 (1989).
- Sciorati, C. *et al.* Fat deposition and accumulation in the damaged and inflamed skeletal muscle: Cellular and molecular players. *Cell Mol. Life Sci.* **72**(11), 2135–2156 (2015).
- Arner, P. & Ryden, M. The contribution of bone marrow-derived cells to the human adipocyte pool. *Adipocyte* **6**(3), 187–192 (2017).
- Schubel, R. *et al.* Key genes of lipid metabolism and WNT-signaling are downregulated in subcutaneous adipose tissue with moderate weight loss. *Nutrients* **11**(3), 639 (2019).
- Zeng, H. *et al.* MicroRNA-339 inhibits human hepatocellular carcinoma proliferation and invasion via targeting ZNF689. *Drug Des. Dev. Ther.* **13**, 435–445 (2019).
- Wang, B. *et al.* Nutrigenomic regulation of adipose tissue development—Role of retinoic acid: A review. *Meat Sci.* **120**, 100–106 (2016).

14. Jiang, S. *et al.* Transcriptome comparison between porcine subcutaneous and intramuscular stromal vascular cells during adipogenic differentiation. *PLoS ONE* **8**(10), e77094 (2013).
15. Poulos, S. P. & Hausman, G. J. A comparison of thiazolidinedione-induced adipogenesis and myogenesis in stromal-vascular cells from subcutaneous adipose tissue or semitendinosus muscle of postnatal pigs. *J. Anim. Sci.* **84**(5), 1076–1082 (2006).
16. Li, A. *et al.* Identification and characterization of circRNAs of two pig breeds as a new biomarker in metabolism-related diseases. *Cell Physiol. Biochem.* **47**(6), 2458–2470 (2018).
17. Sanger, H. L. *et al.* Viroids are single-stranded covalently closed circular RNA molecules existing as highly base-paired rod-like structures. *Proc. Natl. Acad. Sci. USA* **73**(11), 3852–3856 (1976).
18. Memczak, S. *et al.* Circular RNAs are a large class of animal RNAs with regulatory potency. *Nature* **495**(7441), 333–338 (2013).
19. Bozzoni, I. Widespread occurrence of circular RNA in eukaryotes. *Nat. Rev. Genet.* **22**(9), 550–551 (2021).
20. Li, Y. *et al.* Accurate identification of circRNA landscape and complexity reveals their pivotal roles in human oligodendroglia differentiation. *Genome Biol.* **23**(1), 48 (2022).
21. Zhang, S. *et al.* Characterization of circRNA-associated-ceRNA networks in a senescence-accelerated mouse prone 8 brain. *Mol. Ther.* **25**(9), 2053–2061 (2017).
22. Ashwal-Fluss, R. *et al.* circRNA biogenesis competes with pre-mRNA splicing. *Mol. Cell* **56**(1), 55–66 (2014).
23. Dong, R. *et al.* Increased complexity of circRNA expression during species evolution. *RNA Biol.* **14**(8), 1064–1074 (2017).
24. Ozdemir, S. & Arslan, H. circRNA-based biomarker candidates for acute cypermethrin and chlorpyrifos toxication in the brain of zebrafish (*Danio rerio*). *Chemosphere* **298**, 134330 (2022).
25. Sharma, P. *et al.* Generation of transgenic rice expressing circRNA and its functional characterization. *Methods Mol. Biol.* **2362**, 35–68 (2021).
26. Glazar, P., Papavasileiou, P. & Rajewsky, N. circBase: A database for circular RNAs. *RNA* **20**(11), 1666–1670 (2014).
27. Hansen, T. B. *et al.* Natural RNA circles function as efficient microRNA sponges. *Nature* **495**(7441), 384–388 (2013).
28. Du, W. W. *et al.* Identifying and characterizing circRNA-protein interaction. *Theranostics* **7**(17), 4183–4191 (2017).
29. Dube, U. *et al.* An atlas of cortical circular RNA expression in Alzheimer disease brains demonstrates clinical and pathological associations. *Nat. Neurosci.* **22**(11), 1903–1912 (2019).
30. Tang, Q. & Hann, S. S. Biological roles and mechanisms of circular RNA in human cancers. *Onco Targets Ther.* **13**, 2067–2092 (2020).
31. Zhang, S. *et al.* Circular RNA circ\_0003204 inhibits proliferation, migration and tube formation of endothelial cell in atherosclerosis via miR-370-3p/TGFBetaR2/phosph-SMAD3 axis. *J. Biomed. Sci.* **27**(1), 11 (2020).
32. Zhou, Z. B. *et al.* Silencing of circ.RNA2837 plays a protective role in sciatic nerve injury by sponging the miR-34 family via regulating neuronal autophagy. *Mol. Ther. Nucleic Acids* **12**, 718–729 (2018).
33. Dong, W. *et al.* The RNA-binding protein RBM3 promotes cell proliferation in hepatocellular carcinoma by regulating circular RNA SCD-circRNA 2 production. *EBioMedicine* **45**, 155–167 (2019).
34. Ragusa, M. *et al.* CircNAPEPLD is expressed in human and murine spermatozoa and physically interacts with oocyte miRNAs. *RNA Biol.* **16**(9), 1237–1248 (2019).
35. Liu, K. S. *et al.* Biological functions of circular RNAs and their roles in occurrence of reproduction and gynecological diseases. *Am. J. Transl. Res.* **11**(1), 1–15 (2019).
36. Gao, Y., Wang, J. & Zhao, F. CIRI: An efficient and unbiased algorithm for de novo circular RNA identification. *Genome Biol.* **16**, 4 (2015).
37. Anders, S. & Huber, W. Differential expression analysis for sequence count data. *Genome Biol.* **11**(10), R106 (2010).
38. Quan, L. *et al.* Identification of target genes regulated by KSHV miRNAs in KSHV-infected lymphoma cells. *Pathol. Oncol. Res.* **21**(4), 875–880 (2015).
39. Ebbesen, K. K., Hansen, T. B. & Kjems, J. Insights into circular RNA biology. *RNA Biol.* **14**(8), 1035–1045 (2017).
40. John, B. *et al.* Human microRNA targets. *PLoS Biol.* **2**(11), e363 (2004).
41. Yu, G. *et al.* clusterProfiler: An R package for comparing biological themes among gene clusters. *OMICS* **16**(5), 284–287 (2012).
42. Livak, K. J. & Schmittgen, T. D. *Analysis of Relative Gene Expression Data Using Real-Time Quantitative PCR and the 2<sup>-Delta Delta C(T)</sup> Method.* (2013).
43. Prats, A. C. *et al.* Circular RNA, the key for translation. *Int. J. Mol. Sci.* **21**(22), 8591 (2020).
44. Guo, J. U. *et al.* Expanded identification and characterization of mammalian circular RNAs. *Genome Biol.* **15**(7), 409 (2014).
45. Chandrasinghe, P. *et al.* Role of SMAD proteins in colitis-associated cancer: From known to the unknown. *Oncogene* **37**(1), 1–7 (2018).
46. Lee, M. J. Transforming growth factor beta superfamily regulation of adipose tissue biology in obesity. *Biochim. Biophys. Acta Mol. Basis Dis.* **1864**(4 Pt A), 1160–1171 (2018).
47. Budi, E. H., Duan, D. & Derynck, R. Transforming growth factor-beta receptors and smads: Regulatory complexity and functional versatility. *Trends Cell Biol.* **27**(9), 658–672 (2017).
48. Matsubara, T. *et al.* TGF-beta-SMAD3 signaling mediates hepatic bile acid and phospholipid metabolism following lithocholic acid-induced liver injury. *J. Lipid Res.* **53**(12), 2698–2707 (2012).
49. Xiao, J. *et al.* miR-212 downregulation contributes to the protective effect of exercise against non-alcoholic fatty liver via targeting FGF-21. *J. Cell Mol. Med.* **20**(2), 204–216 (2016).
50. Xiao, J. *et al.* miR-149 controls non-alcoholic fatty liver by targeting FGF-21. *J. Cell Mol. Med.* **20**(8), 1603–1608 (2016).
51. Chen, T. *et al.* The effect of microRNA-331-3p on preadipocytes proliferation and differentiation and fatty acid accumulation in Laiwu pigs. *Biomed. Res. Int.* **2019**, 9287804 (2019).
52. Salama, I. I. *et al.* Plasma microRNAs biomarkers in mild cognitive impairment among patients with type 2 diabetes mellitus. *PLoS ONE* **15**(7), e0236453 (2020).
53. Pan, S. *et al.* MicroRNA-128 is involved in dexamethasone-induced lipid accumulation via repressing SIRT1 expression in cultured pig preadipocytes. *J. Steroid Biochem. Mol. Biol.* **186**, 185–195 (2019).
54. Wang, J. *et al.* Comprehensive analysis of differentially expressed mRNA, lncRNA and circRNA and their ceRNA networks in the longissimus dorsi muscle of two different pig breeds. *Int. J. Mol. Sci.* **20**(5), 1107 (2019).
55. Petan, T., Jarc, E. & Jusovic, M. Lipid droplets in cancer: Guardians of fat in a stressful world. *Molecules* **23**(8), 1941 (2018).
56. Santasusagna, S. *et al.* miR-328 mediates a metabolic shift in colon cancer cells by targeting SLC2A1/GLUT1. *Clin. Transl. Oncol.* **20**(9), 1161–1167 (2018).
57. Saberi, A. *et al.* MiR-328 may be considered as an oncogene in human invasive breast carcinoma. *Iran Red Crescent. Med. J.* **18**(11), e42360 (2016).
58. Qin, X. & Guo, J. MicroRNA-328-3p protects vascular endothelial cells against oxidized low-density lipoprotein induced injury via targeting forkhead box protein O4 (FOXO4) in atherosclerosis. *Med. Sci. Monit.* **26**, e921877 (2020).
59. Wu, C. Y. *et al.* MicroRNA-328 ameliorates oxidized low-density lipoprotein-induced endothelial cells injury through targeting HMGB1 in atherosclerosis. *J. Cell Biochem.* **120**, 1643–1650 (2018).
60. Xie, W. *et al.* Beneficial role of microRNA-328-3p in fracture healing by enhancing osteoblastic viability through the PTEN/PI3K/AKT pathway. *Exp. Ther. Med.* **20**(6), 271 (2020).
61. Oliverio, M. *et al.* Dicer1-miR-328-Bace1 signalling controls brown adipose tissue differentiation and function. *Nat. Cell Biol.* **18**(3), 328–336 (2016).

62. Cazanave, S. C. *et al.* A role for miR-296 in the regulation of lipopoptosis by targeting PUMA. *J. Lipid Res.* **52**(8), 1517–1525 (2011).
63. Belarbi, Y. *et al.* MicroRNAs-361-5p and miR-574-5p associate with human adipose morphology and regulate EBF1 expression in white adipose tissue. *Mol. Cell Endocrinol.* **472**, 50–56 (2018).
64. Lefterova, M. I. & Lazar, M. A. New developments in adipogenesis. *Trends Endocrinol. Metab.* **20**(3), 107–114 (2009).
65. Katoh, M. & Katoh, M. WNT signaling pathway and stem cell signaling network. *Clin. Cancer Res.* **13**(14), 4042–4045 (2007).
66. Otto, T. C. & Lane, M. D. Adipose development: from stem cell to adipocyte. *Crit. Rev. Biochem. Mol. Biol.* **40**(4), 229–242 (2005).
67. Takada, I. *et al.* A histone lysine methyltransferase activated by non-canonical Wnt signalling suppresses PPAR-gamma transactivation. *Nat. Cell Biol.* **9**(11), 1273–1285 (2007).
68. Kanazawa, A. *et al.* Wnt5b partially inhibits canonical Wnt/beta-catenin signaling pathway and promotes adipogenesis in 3T3-L1 preadipocytes. *Biochem. Biophys. Res. Commun.* **330**(2), 505–510 (2005).
69. Wang, Y. X. *et al.* Peroxisome-proliferator-activated receptor delta activates fat metabolism to prevent obesity. *Cell* **113**(2), 159–170 (2003).
70. Tanaka, T. *et al.* Activation of peroxisome proliferator-activated receptor delta induces fatty acid beta-oxidation in skeletal muscle and attenuates metabolic syndrome. *Proc. Natl. Acad. Sci. U S A* **100**(26), 15924–15929 (2003).
71. Luquet, S. *et al.* Roles of PPAR delta in lipid absorption and metabolism: A new target for the treatment of type 2 diabetes. *Biochim. Biophys. Acta* **1740**(2), 313–317 (2005).
72. Yu, Y. H. *et al.* Ectopic expression of porcine peroxisome proliferator-activated receptor delta regulates adipogenesis in mouse myoblasts. *J. Anim. Sci.* **86**(1), 64–72 (2008).
73. Odegaard, J. I. *et al.* Alternative M2 activation of Kupffer cells by PPARdelta ameliorates obesity-induced insulin resistance. *Cell Metab.* **7**(6), 496–507 (2008).
74. Brestoff, J. R. *et al.* Intercellular mitochondria transfer to macrophages regulates white adipose tissue homeostasis and is impaired in obesity. *Cell Metab.* **33**(2), 270–2828 (2021).
75. Han, J. K. *et al.* Peroxisome proliferator-activated receptor-delta activates endothelial progenitor cells to induce angio-myogenesis through matrix metallo-proteinase-9-mediated insulin-like growth factor-1 paracrine networks. *Eur. Heart J.* **34**(23), 1755–1765 (2013).
76. Wang, L. & Shan, T. Factors inducing transdifferentiation of myoblasts into adipocytes. *J. Cell Physiol.* **236**(4), 2276–2289 (2021).
77. Kotlinowski, J. & Jozkowicz, A. PPAR gamma and angiogenesis: Endothelial cells perspective. *J. Diabetes Res.* **2016**, 8492353 (2016).
78. Hurt, B. *et al.* Cancer-promoting mechanisms of tumor-associated neutrophils. *Am. J. Surg.* **214**(5), 938–944 (2017).
79. Mazzotti, D. R. *et al.* Association of APOE, GCPII and MMP9 polymorphisms with common diseases and lipid levels in an older adult/elderly cohort. *Gene* **535**(2), 370–375 (2014).
80. Stephens, D. C. *et al.* Imaging the rapid yet transient accumulation of regulatory lipids, lipid kinases, and protein kinases during membrane fusion, at sites of exocytosis of MMP-9 in MCF-7 cells. *Lipids Health Dis.* **19**(1), 195 (2020).
81. Allott, E. H. *et al.* MMP9 expression in oesophageal adenocarcinoma is upregulated with visceral obesity and is associated with poor tumour differentiation. *Mol. Carcinog.* **52**(2), 144–154 (2013).
82. Ii, H. *et al.* Group IVA phospholipase A2-associated production of MMP-9 in macrophages and formation of atherosclerotic lesions. *Biol. Pharm. Bull.* **31**(3), 363–368 (2008).
83. Zhang, N. *et al.* Ketogenic diet elicits antitumor properties through inducing oxidative stress, inhibiting MMP-9 expression, and rebalancing M1/M2 tumor-associated macrophage phenotype in a mouse model of colon cancer. *J. Agric. Food Chem.* **68**(40), 11182–11196 (2020).
84. Thamer, C. *et al.* Variations in PPAR delta determine the change in body composition during lifestyle intervention: A whole-body magnetic resonance study. *J. Clin. Endocrinol. Metab.* **93**(4), 1497–1500 (2008).
85. Scott, L. J. *et al.* A genome-wide association study of type 2 diabetes in Finns detects multiple susceptibility variants. *Science* **316**(5829), 1341–1345 (2007).
86. Lu, L. *et al.* Associations of type 2 diabetes with common variants in PPAR delta and the modifying effect of vitamin D among middle-aged and elderly Chinese. *PLoS ONE* **7**(4), e34895 (2012).
87. Zhang, Y. *et al.* The functional SNPs in the 5' regulatory region of the porcine PPAR delta gene have significant association with fat deposition traits. *PLoS ONE* **10**(11), e0143734 (2015).

## Author contributions

X.Y.M. conceived, designed and performed the experiments and wrote the paper; H.F. performed the experiment and data analysis and wrote the paper; T.Y.L., S.Y., X.Z., W.H., A.L. and L.X. performed the experiments. All authors read and approved the final manuscript.

## Funding

This work was supported the National Natural Science Foundation of China (No. 31970541), The Major Science and Technology Project of New Variety Breeding of Genetically Modified Organisms (Nos. 2009ZX08008-004B and 2008ZX08008-003), the Agricultural Science and Technology Innovation Program (NO. ASTIP-IAS05), the Basic Research Fund for Central Public Research Institutes of CAAS (Y2016JC22, Y2018PT68), and the Basic Research Fund for Central Public Research Institutes of CAAS (2013ywf-yb-5, 2013ywf-zd-2).

## Competing interests

The authors declare no competing interests.

## Additional information

**Supplementary Information** The online version contains supplementary material available at <https://doi.org/10.1038/s41598-022-21045-2>.

**Correspondence** and requests for materials should be addressed to X.M.

**Reprints and permissions information** is available at [www.nature.com/reprints](http://www.nature.com/reprints).

**Publisher's note** Springer Nature remains neutral with regard to jurisdictional claims in published maps and institutional affiliations.



**Open Access** This article is licensed under a Creative Commons Attribution 4.0 International License, which permits use, sharing, adaptation, distribution and reproduction in any medium or format, as long as you give appropriate credit to the original author(s) and the source, provide a link to the Creative Commons licence, and indicate if changes were made. The images or other third party material in this article are included in the article's Creative Commons licence, unless indicated otherwise in a credit line to the material. If material is not included in the article's Creative Commons licence and your intended use is not permitted by statutory regulation or exceeds the permitted use, you will need to obtain permission directly from the copyright holder. To view a copy of this licence, visit <http://creativecommons.org/licenses/by/4.0/>.

© The Author(s) 2022